

Computation of vector hazard using salient features of seismic hazard deaggregation

Somayajulu L. N. Dhulipala^{a)} S.M.EERI, Adrian Rodriguez-Marek^{a)} M.EERI and Madeleine M. Flint^{a)} M.EERI

Deaggregation is one of the products of Probabilistic Seismic Hazard Analysis suitable for identifying the relative contributions of various magnitude-distance bins to a hazard or Intensity Measure (IM) level. In this paper, we elucidate some interesting features of deaggregations such as: their monotonically decreasing nature with IM; their invariance to any minimum IM level; and the pertinence of their bins to a complementary cumulative distribution function. We use these features of hazard deaggregation along with Copula functions in a simplified method for computing vector deaggregation and vector hazard given the scalar counterparts. We validate our simplified procedure at a hypothetical site surrounded by multiple fault sources where seismic hazard is calculated using a logic-tree. We also demonstrate the application of our approach to a real site in Los Angeles, CA. Finally, we explore whether the invariance property of deaggregations can be used to compute scalar hazard curves using new Ground Motion Prediction Models/IMs and find that for low to moderate levels of IM, a reasonable approximation is obtained.

INTRODUCTION

Deaggregation is one of the products of Probabilistic Seismic Hazard Analysis (PSHA) that aids in the identification of the relative importance of different Magnitude (M) and Distance (R) values given an earthquake Intensity Measure (IM) level. Following Bazzurro and Cornell (1999), it is typical to represent deaggregation plots as percentage contribution to hazard (or simply conditional probability) versus various M-R combinations. These plots have been widely used to identify a design earthquake scenario and to generate spectra for ground motion selection such as the Conditional Mean Spectrum (CMS). Deaggregations have three interesting properties in relation to vector hazard/deaggregation computations: a) the product of deaggregation probability and Annual Frequency of Exceedance (AFE) decreases monotonically with the IM level; b) they are invariant to the choice of IM for a reasonably low IM level; c) the probability mass

^{a)}Department of Civil and Environmental Engineering, Virginia Tech, Blacksburg, VA (lakshd5@vt.edu)

given an M-R combination is actually part of a Complementary Cumulative Distribution Function (CCDF), which will be termed the aggregated conditional probability of IM exceedence for reasons specified later. These properties can be used to obtain, in a simplified way, vector hazard curve and deaggregation while the obeying logic tree and fault-specific parameters of the multiple seismic sources considered. Vector hazard has applications in seismic demand hazard analysis considering a vector of IMs (Kohrangi et al., 2016b). Vector deaggregation is also required to generate the conditional mean spectrum conditioned on multiple IMs (Kwong and Chopra, 2016).

In this paper, we first elucidate the above-mentioned properties in detail and mathematically formalize them. Next, we exploit these properties of deaggregations to derive the vector deaggregation and hazard for a suite of IMs. In particular, given an M-R combination and aggregated conditional probability of IM exceedence corresponding to two (or more) IMs, the joint aggregated conditional probability of IM exceedences can be derived using Copulas. The vector deaggregation and hazard can then be conveniently recovered by invoking the invariance property of deaggregations. We validate our simplified procedure at a hypothetical site surrounded by multiple fault sources where seismic hazard is calculated using a logic-tree. We also demonstrate the application of our approach to a real site in Los Angeles, CA using the outputs from the PSHA program OpenSHA (Field et al., 2003). Additionally, we also explore whether the invariance property of deaggregations can be used to compute scalar hazard curves using new GMPMs/IMs.

PRIOR RESEARCH ON VECTOR HAZARD ANALYSIS

Vector PSHA has received considerable attention since the seminal paper by Bazzurro and Cornell (2002). This interest can be partly attributed to the anticipation that a vector of IMs can better predict structural demand than a scalar IM. Consequently, researchers have proposed simplified methods to perform vector PSHA calculations without re-running the computationally expensive seismic hazard analyses. Bazzurro et al. (2009) and ? propose a simplified ‘indirect’ approach to perform vector PSHA using the results of scalar seismic hazard analyses. Their approach splits the joint probability of exceedence of multiple IMs into conditional densities and evaluates each conditional density individually. Along similar lines, Barbosa (2011) uses this ‘indirect’ method to compute seismic hazard and deaggregation for a suite of three IMs. Kohrangi et al. (2016a), from a practical viewpoint, note that this ‘indirect’ approach for vector PSHA has two limitations in relation to modern seismic hazard analysis: (1) it does not respect

the logic-tree used in most PSHA applications and (2) it cannot consider the fault-specific characteristics of the different seismic sources analyzed. If the ‘indirect’ technique is to be applied while considering the above two attributes, then hazard deaggregation outputs from PSHA programs would need to provide information related to logic-tree branch weights as well as the multitude of fault-specific parameters^{a)}. Because most contemporary PSHA programs provide deaggregation matrices that only describe the probability mass distribution of various M-R combinations conditional on an IM level, the ‘indirect’ technique for Vector PSHA is therefore limited in application in the context of modern PSHA standards. Additionally, the consequences of using the ‘indirect’ technique for case-studies considering logic-tree and multiple seismic sources with specific fault parameters have not been investigated.

OBJECTIVES OF THE PRESENT STUDY

Enabling existing PSHA programs (e.g., OpenSHA, the USGS hazard tool, and the OpenQuake engine) to perform an exact vector hazard analysis requires modifications to their code-bases, which on its own can be a substantial project. This short-coming has significantly limited the utilization of vector PSHA in Performance Based Earthquake Engineering practice (Bazzurro and Park, 2011; Kohrangi et al., 2016a). Hence, in order to provide an efficient, effective, and a pre-configured solution to the problem of Vector PSHA that is consistent with modern PSHA standards, the goal of this paper is to compute vector hazard using only the basic outputs of most existing PSHA programs that an analyst can retrieve: scalar hazard curves and M-R deaggregation matrices. This paper proposes a novel simplification to vector hazard analysis that considers logic-tree and fault-specific parameters, and in doing so, identifies important features of scalar seismic hazard deaggregations that enable the use of Copula functions in computing the vector hazard. A MATLAB routine is developed that takes inputs as M-R deaggregation matrices, scalar hazard values (obtained from a PSHA program), and correlations between N IMs to return vector hazard/deaggregation.

BACKGROUND

Consider a site surrounded by N_s earthquake sources. For various combinations of magnitude (M), distance (R) and other source/site parameters (\hat{p}), the Annual Frequency of Exceedance (AFE) of an earthquake Intensity Measure (IM) level is expressed as (Lin, 2012)

^{a)}In such cases, the computational expense of the ‘indirect’ approach is nearly equivalent to performing an exact vector PSHA.

$$\lambda(IM > x) = \sum_{i=1}^{Ns} \lambda_{0i} \sum_{j=1}^{N_{MR}} \sum_{k=1}^{N_{LT}} w_k \left[\int_{\varepsilon} P(IM > x | M_{jk}, R_{jk}, \hat{p}_{ik}, \varepsilon) f(\varepsilon) d\varepsilon \right] P(M_{ijk}, R_{ijk}) \quad (1)$$

where λ_{0i} is the AFE of the minimum earthquake for the i^{th} earthquake source, w_k is the weight given to the k^{th} logic tree branch, \hat{p}_{ik} is a vector of source/site parameters dependent on i^{th} source and k^{th} logic tree branch, $P(M_{ijk}, R_{ijk})$ is the probability of the j^{th} M-R combination under i^{th} earthquake source and k^{th} logic tree branch, parameter ε is the normalized residuals between natural logarithms of observed and predicted ground motion and $f(\varepsilon)$ is its probability density function. N_{MR} and N_{LT} are the number of M-R bins and logic tree branches, respectively. It is noted that logic-tree weights (w_k) can be assigned to various types of assumptions, including multiple GMPM models, limits on maximum magnitude, or fault types. The weights thereby influence $P(IM > x | M_{jk}, R_{jk}, \hat{p}_{ik}, \varepsilon)$ and $P(M_{ijk}, R_{ijk})$ in equation (1). The IM exceedence probability conditional on various parameters is computed as

$$P(IM > x | M_{jk}, R_{jk}, \hat{p}_{ik}, \varepsilon) = 1 - \Phi \left(\frac{\ln x - (\mu(M_{jk}, R_{jk}, \hat{p}_{ik}) + \varepsilon \sigma_{\ln IM})}{\sigma_{\ln IM}} \right) \quad (2)$$

where $\Phi(\cdot)$ is the standard normal cumulative distribution function, $\mu(M_{jk}, R_{jk}, \hat{p}_{ik})$ is the natural logarithm of the median IM prediction obtained from a GMPM in the logic tree and $\sigma_{\ln IM}$ is the model standard deviation. If the fractional contribution to hazard from a particular M-R combination is desired, we perform hazard deaggregation using Bayes' rule (Hoff, 2009)

$$P(M_j, R_j | IM > x) = \frac{\lambda(IM > x, M_j, R_j)}{\lambda(IM > x)} \quad (3)$$

where $\lambda(IM > x, M_j, R_j)$ is the rate of earthquakes with $IM > x$, $M = M_j$ and $R = R_j$. It is noted that the numerator in the above equation is a subset of the sample space with specific values of M-R, while the denominator is the entire sample space. $\lambda(IM > x, M_j, R_j)$ can be further expressed as

$$\lambda(IM > x, M_j, R_j) = \sum_{i=1}^{Ns} \lambda_{0i} \sum_{k=1}^{N_{LT}} w_k P(IM > x | M_{jk}, R_{jk}, \hat{p}_{ik}) P(M_{ijk}, R_{ijk}) \quad (4)$$

where $P(IM > x | M_{jk}, R_{jk}, \hat{p}_{ik})$ is obtained by integrating over all possible values of ε represented by terms in the square bracket in equation (1).

EXAMPLE SEISMIC HAZARD ANALYSIS FOR A HYPOTHETICAL SITE

A hypothetical site (located at the origin $(0, 0)$) surrounded by two faults modeled as line sources will be used to perform a scalar seismic hazard analysis, and also to demonstrate the vector hazard and deaggregation procedure proposed in this paper. A truncated Gutenberg-Richter model is used to construct a probability distribution for magnitudes, and a simple point model is adopted to account for the uncertainty in hypocenter location. Point models consider the uncertainty only in the rupture initiation point without regard to the uncertainty in rupture length (Kramer, 1996). Epsilons are not truncated for the seismic hazard computations at this site. The average shear wave velocity over the top thirty meters (V_{s30}) is assumed to be 400 m/s. Other fault parameters that will be relevant for modeling purposes are provided in Table 1.

Table 1. List of parameters for the two faults near the hypothetical site $(0, 0)$

Property	Line source 1	Line source 2
Coordinates	$(-20, -15)$ $(12, -10)$	$(-35, 20)$ $(20, 30)$
R_{min} (Km)	11.732	25.938
R_{max} (Km)	25	40.311
'a'	2	1.5
'b'	0.8	1
λ_0	0.063	0.00316
δ	75°	75°
λ	90° (R), -90° (N)	90° (R), -90° (N)
Z_{tor} (Km)	0	1
Z_{vs} (Km)	2	2

Abbreviations. R_{min} : Minimum distance; R_{max} : Maximum distance; 'a': Gutenberg-Richter parameter; 'b': Gutenberg-Richter parameter; λ_0 : AFE of the minimum earthquake; δ : Dip angle; λ : Rake angle; Z_{tor} : Depth to top of the co-seismic rupture; Z_{vs} : Depth to the 2.5 km/s shear-wave velocity horizon; R: Reverse fault; N: Normal fault.

A logic-tree is used for this hypothetical site to capture the epistemic uncertainty associated with establishing maximum magnitudes, GMPM selection, and fault type. The logic-tree comprises eight final branches, with two options each for: maximum magnitude ($M_{max} = 7$ or 7.5), GMPM (either Campbell and Bozorgnia (2008) or Boore and Atkinson (2008)), and fault-type (either Reverse or Normal faulting mechanism). A depiction of this logic-tree is provided in Figure 1 along with the weights given to each of its branches.

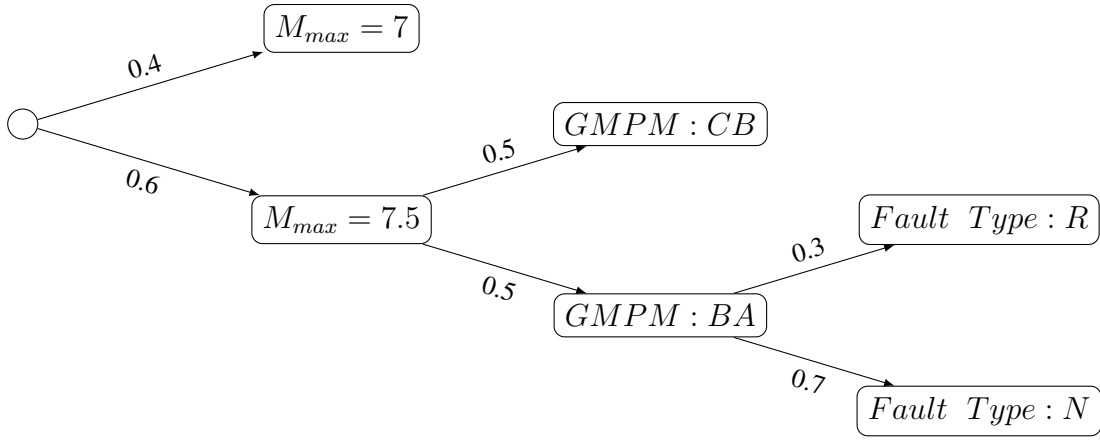


Figure 1. Depiction of the logic-tree used for the hypothetical site considered in this study. Only unique branches arising at each rightward step are represented (there are eight final branches). A fraction along each of the branch arrows represents the weight given to that rightward step. Abbreviations: Campbell-Bozorgnia 2008 (*CB*), Boore-Atkinson 2008 (*BA*), Reverse fault (*R*), Normal fault (*N*).

128 Figure 2a provides the seismic hazard curves for the IM $Sa(2s)$ computed under the stan-
 129 dard PSHA using a logic-tree approach; both the individual logic-tree branches and the final
 130 weighted curve are provided. Figure 2b provides a deaggregation plot at for $Sa(2s) > 0.5g$,
 131 where the M and the R are discretized into twenty bins each.

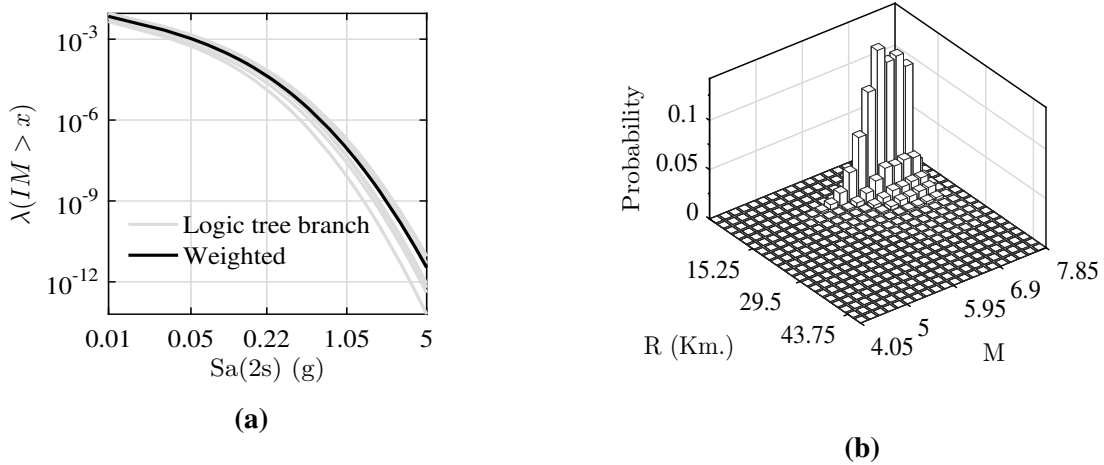


Figure 2. (a) Seismic hazard curves at hypothetical site for the IM $Sa(2s)$ (b) Hazard deaggregation at $Sa(2s) > 0.5g$.

132 FEATURES OF SEISMIC HAZARD DEAGGREGATION

133 The expression of the numerator in equation (3) as a joint frequency, rather than a product of
 134 conditional probability of IM exceedance and probability mass of an M-R combination, allows

us to elucidate three key features of deaggregations. These features then enable a direct computation of vector deaggregation and hence vector hazard as discussed later.

a) *Monotonically decreasing nature with IM level*

For a particular M-R bin, re-arranging equation (3) gives

$$\lambda(IM > x, M_j, R_j) = P(M_j, R_j | IM > x) \lambda(IM > x) \quad (5)$$

The right hand side of the above equation can be computed given the scalar hazard curve and deaggregation at an IM level. It is evident that the above equation monotonically decreases with IM level: for a fixed M-R, $P(IM > x | M_{jk}, R_{jk}, \hat{p}_{ik})$ corresponds to a CCDF and hence should decrease as the IM level increases, thus $\lambda(IM > x, M_j, R_j)$ should also decrease as the IM level increases (see equation (4)). Figure 3 provides examples of the $\lambda(IM > x, M_j, R_j)$ function (equation (5)) with IM level for the two M-R combinations at the hypothetical site.

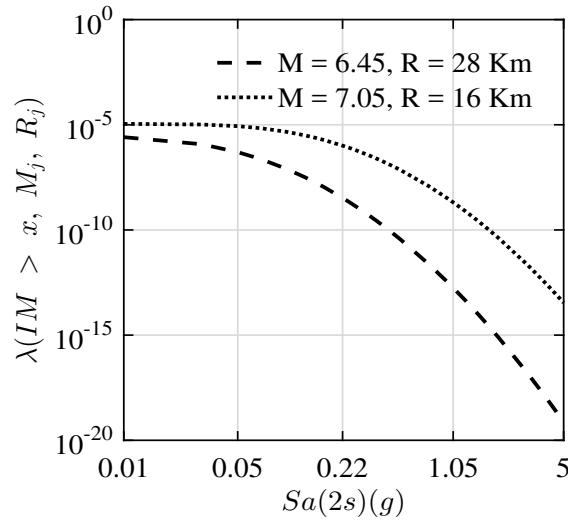


Figure 3. $\lambda(IM > x, M_j, R_j)$ with $Sa(2s)$ level for M-R bins (6.45, 28Km) and (7.05, 16Km), respectively, depicting the function's monotonically decreasing nature.

The monotonically decreasing nature of deaggregation matrices highlights the fact that these matrices are also a function of IM level. This will enable us to derive a quantity, termed the *aggregate conditional probability of IM exceedence*, later on that eases the computation of vector hazard/deaggregation.

b) *Invariance to any minimum IM level*

150 A second interesting property of deaggregations is their invariance to the choice of IM
 151 for a low IM level. If in equation (4), the IM level selected is sufficiently low, $P(IM >$
 152 $x|M_{jk}, R_{jk}, \hat{p}_{ik})$ would be unity for all M-R combinations: i.e., all earthquakes must cause at
 153 least some ground motion. Then equations (4) or (5) would simply represent the distribution of
 154 M-R and hence be invariant to any choice of IM. This is mathematically expressed as

$$\lambda(IM_1 > x_{min}, M_j, R_j) = \lambda(IM_2 > y_{min}, M_j, R_j) = \lambda(M_j, R_j) \quad (6)$$

155 where x_{min} and y_{min} are minimum levels for the IMs IM_1 and IM_2 respectively. Figure 4
 156 provides, for the hypothetical site, the equivalence of deaggregations for the IMs Sa(2s) and
 157 PGA at a level of $10^{-6}g$ each.

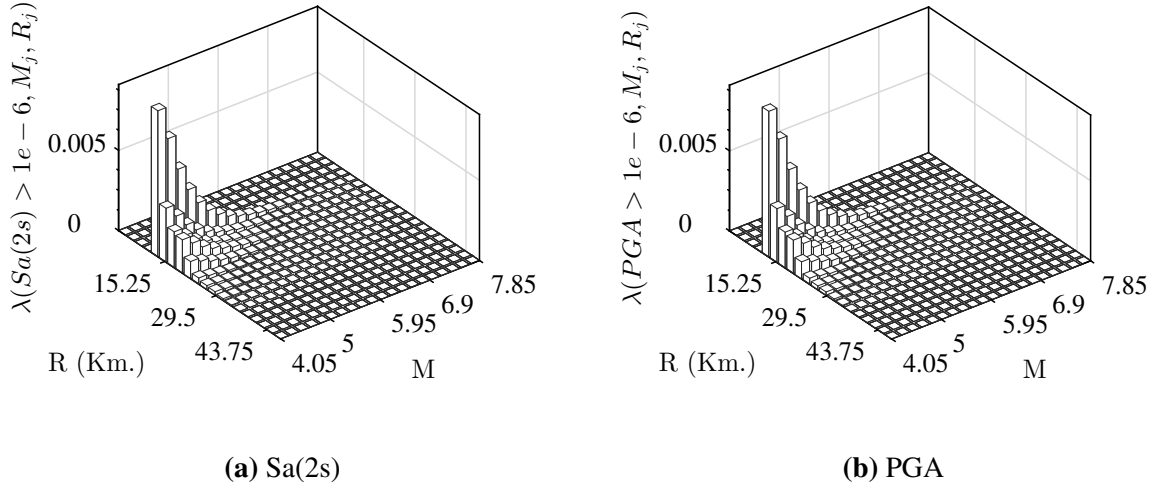


Figure 4. Invariance of deaggregations with the choice of IM for a low IM level ($1e-6$ g)

158 It is noted that equations (5) and (6) enable the user to retrieve a discrete form of the initial
 159 M-R distribution that goes into hazard calculations. Such a discretized unconditional M-R dis-
 160 tribution, as will be evident later, also conveniently lends itself to vector hazard computations.

161 *c) Each M-R bin pertains to a CCDF of the IM*

162 The final relevant property of deaggregations is that each M-R bin is part of a CCDF of the
 163 IM. Using Bayes' rule, the fractional contribution to an IM exceedence conditional on M-R can
 164 be expressed as

$$P_A(IM > x|M_j, R_j) \equiv \frac{\lambda(IM > x, M_j, R_j)}{\lambda(M_j, R_j)} \quad (7)$$

165 where the numerator is obtained from equation (5) and the denominator, which represents the
 166 rate of earthquakes with $M = M_j$ and $R = R_j$ is obtained from equation (6). In other words,
 167 deaggregation plots, although normally viewed as function of M-R given an IM level, can be
 168 transformed to be a function of IM exceedence level given an M-R bin, and each bin of the
 169 deaggregation can be related to a CCDF of the IM via Bayes' rule. Equation (7) can be expanded
 170 as

$$P_A(IM > x | M_j, R_j) = \frac{\sum_{i=1}^{N_s} \lambda_{0i} \sum_{k=1}^{N_{LT}} w_k P(IM > x | M_{jk}, R_{jk}, \hat{p}_{ik}) P(M_{ijk}, R_{ijk})}{\sum_{i=1}^{N_s} \lambda_{0i} \sum_{k=1}^{N_{LT}} w_k P(M_{ijk}, R_{ijk})} \quad (8)$$

171 from which it can be noticed that contributions from all logic-tree branches and seismic sources
 172 are considered. Because of this attribute of equations (7) and (8), $P_A(IM > x | M_j, R_j)$ will be
 173 termed the *aggregated conditional probability of IM exceedence*.

174 Figure 5 provides aggregate conditional probability of IM exceedence for Sa(2s) conditional
 175 on two M-R combinations.

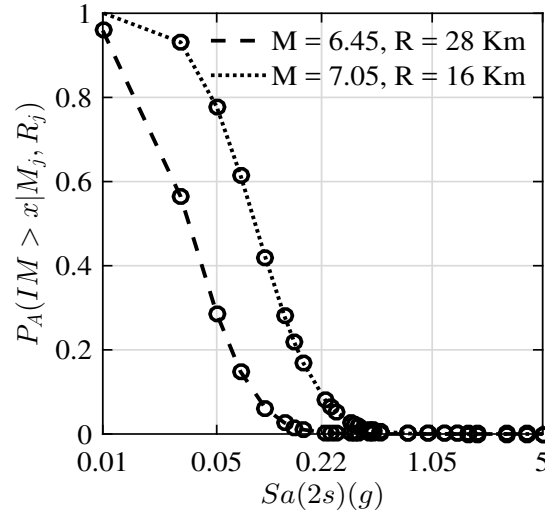


Figure 5. Aggregated conditional probability of IM exceedence for the IM Sa(2s) conditional on M-R bins (6.45, 28Km) and (7.05, 16Km), respectively, at the hypothetical site

176 Using the aggregate conditional probability of IM exceedence, the scalar hazard curve can
 177 be directly recovered while still adhering to a logic tree approach

$$\lambda(IM > x) = \sum_{j=1}^{N_{MR}} P_A(IM > x | M_j, R_j) \lambda(M_j, R_j) \quad (9)$$

178 The above equation is exactly same as equation (1) but both terms on the right hand side
 179 are obtained directly from deaggregation. This equivalence will be evident when the aggregate
 180 conditional probability of IM exceedence is expanded by substituting the definition of
 181 $P_A(IM > x|M_j, R_j)$ (equation (8)) into equation (9),

$$\lambda(IM > x) = \sum_{j=1}^{N_{MR}} \frac{\sum_{i=1}^{N_s} \lambda_{0i} \sum_{k=1}^{N_{LT}} w_k P(IM > x|M_{jk}, R_{jk}, \hat{p}_{ik}) P(M_{ijk}, R_{ijk})}{\lambda(M_j, R_j)} \lambda(M_j, R_j) \quad (10)$$

182 which is same as equation (1) except that the integration with the parameter ε has been sup-
 183 pressed for brevity and the order of summation has been interchanged. The aggregate condi-
 184 tional probability of IM exceedence, although having a similar mathematical notation, is not
 185 equal to the conditional probability of IM level exceedence directly obtained from a GMPM.
 186 The equivalence of these quantities only holds true when a single GMPM is used in the logic
 187 tree and this GMPM does not consider earthquake source related parameters. This is mathe-
 188 matically expressed as

$$P_A(IM > x|M_j, R_j) = \frac{P(IM > x|M_j, R_j, \hat{p}) \sum_{i=1}^{N_s} \lambda_{0i} \sum_{k=1}^{N_{LT}} w_k P(M_{ijk}, R_{ijk})}{\sum_{i=1}^{N_s} \lambda_{0i} \sum_{k=1}^{N_{LT}} w_k P(M_{ijk}, R_{ijk})} \quad (11)$$

189 where $P(IM > x|M_j, R_j, \hat{p})$ in the numerator shows that a single GMPM which is independent
 190 of source parameters has been used (comparing with equation (8)). This condition will be
 191 further explored later in this paper.

192 To obtain a joint hazard/deaggregation conditioned on two or more IM levels, it will be
 193 beneficial to express the aggregate conditional probability of IM exceedence (equation (7)) as a
 194 CDF

$$P_A(IM < x|M_j, R_j) = 1 - P_A(IM > x|M_j, R_j) = 1 - \frac{\lambda(IM > x, M_j, R_j)}{\lambda(M_j, R_j)} \quad (12)$$

195 VECTOR DEAGGREGATION AND VECTOR HAZARD

196 The properties of scalar deaggregation can be utilized, as shown below, to compute the vector
 197 hazard and deaggregation. Let IM_1, \dots, IM_n be the IMs whose joint aggregate conditional

probability of IM non-exceedences given an M-R combination is to be determined. Let the marginal CDFs for these IMs be denoted as $P_A(IM_1 < x|M_j, R_j), \dots, P_A(IM_n < x_n|M_j, R_j)$ respectively. It is noted that under random input of the independent variable (i.e. IM values), CDFs (i.e. $P_A(IM_1 < x|M_j, R_j)$) are uniformly distributed random variables. Sklar's theorem allows the computation of a joint CDF using marginal CDFs (Goda and Atkinson, 2009),

$$\begin{aligned} P_A(IM_1 < x_1, \dots, IM_n < x_n|M_j, R_j) \\ &= C(P_A(IM_1 < x|M_j, R_j), \dots, P_A(IM_n < x_n|M_j, R_j)) \quad (13) \\ &= C(u_1, \dots, u_n) \end{aligned}$$

where C is a Copula function and u denotes a uniformly distributed random variable. A Copula function attempts to capture nonlinear (or non-Gaussian) dependences between random variables through their marginal CDFs. As a result of its aggregation across logic-tree branches and multiple fault sources, the aggregated conditional probability of an IM non-exceedence is likely to be a non-Gaussian marginal. Hence the goal is to compute the non-Gaussian distributed joint aggregated conditional probability of a vector IM non-exceedences through a Copula function and then to use the properties of scalar deaggregations to find the vector hazard/deaggregation.

Despite its name, a Gaussian Copula is frequently preferred to capture nonlinear dependences between random variables owing to its ease-of-use and its acceptable performance (Goda and Atkinson, 2009). This Copula is termed 'Gaussian' due to its reliance on Pearson correlation coefficients to relate the marginal CDFs of two or more random variables arising from arbitrary probability density distributions and its ability to recover a bivariate Gaussian if the marginals of two random variables are Gaussian. Given the correlation matrix between various IMs and uniformly distributed random variables (u_1, \dots, u_n , which represent the aggregated CDFs $P_A(IM_1 < x|M_j, R_j), \dots, P_A(IM_n < x_n|M_j, R_j)$ respectively), a Gaussian copula is defined as

$$C(u_1, \dots, u_n) = \widehat{\Phi}(\Phi^{-1}(u_1), \dots, \Phi^{-1}(u_n)) \quad (14)$$

where Φ^{-1} denotes a scalar inverse standard Gaussian CDF and $\widehat{\Phi}$ is a multivariate Gaussian CDF with a zero mean vector and a covariance matrix equal to the correlation matrix between the IMs. Thus all that is necessary to obtain the vector hazard is the correlation matrix of the IMs. In this paper, it is assumed that the same correlation matrix between the IMs holds for various M-R combinations—an assumption supported by Baker and Bradley (2017) who

conclude that correlations between various IMs show no significant dependence on M-R and site characteristics while using the NGA-West2 database. If other ground motion databases indicate that correlations between IMs are dependent on seismological parameters, then an M-R dependent correlation matrix should be used in equation (14).

Additionally, it is noted that the aggregated conditional probability of a scalar IM exceedence is summed across multiple fault properties and logic-tree branches. We assume that correlation coefficients between IMs are constant across different logic tree branches. This is supported by the observation that these coefficients are not affected by M, R, or site characteristics (Baker and Bradley, 2017). Moreover, Bradley (2011, 2012), **using NGA West 2 GMPMS^{b)}**, showed that correlations between IMs do not change notably with respect to the adopted GMPM. Finally, the authors are not aware of any published literature on the influence of fault characteristics (e.g., fault type, Z_{Tor} , δ) and have assumed that these parameters also do not impact the computed IM correlations.

As we now have the joint CDF (equations (13) and (14)) and the marginal CDFs (equation (12)), we can compute the joint aggregated conditional probability of IM exceedences given a particular M-R bin using De Morgan's law,

$$P_A(IM_1 > x_1, IM_2 > x_2, \dots, IM_n > x_n | M_j, R_j) = 1 - P_A(IM_1 < x_1 \cup IM_2 < x_2 \cup \dots \cup IM_n < x_n | M_j, R_j) \quad (15)$$

For the case of a vector of two IMs, equation (15) can be further written as,

$$\begin{aligned} P_A(IM_1 > x_1, IM_2 > x_2 | M_j, R_j) &= 1 - P_A(IM_1 < x_1 \cup IM_2 < x_2 | M_j, R_j) \\ &= 1 - P_A(IM_1 < x_1 | M_j, R_j) - P_A(IM_2 < x_2 | M_j, R_j) \\ &\quad + P_A(IM_1 < x_1, IM_2 < x_2 | M_j, R_j) \end{aligned} \quad (16)$$

MANIPULATIONS TO COMPUTE THE VECTOR HAZARD/DEAGGREGATION

The joint aggregated conditional probability of IM exceedence can be expanded as

^{b)}These NGA West2 GMPMs include Boore and Atkinson (2008), Campbell and Bozorgnia (2008), Abrahamson and Silva (2008), and Chiou and Youngs (2008). Please refer to an appendix towards the end of this paper for more discussion.

$$P_A(IM_1 > x_1, \dots, IM_n > x_n | M_j, R_j) = \frac{\sum_{i=1}^{N_s} \lambda_{0i} \sum_{k=1}^{N_{LT}} w_k P(IM_1 > x_1, \dots, IM_n > x_n | M_{jk}, R_{jk}, \hat{p}_{ik}) P(M_{ijk}, R_{ijk})}{\sum_{i=1}^{N_s} \lambda_{0i} \sum_{k=1}^{N_{LT}} w_k P(M_{ijk}, R_{ijk})} \quad (17)$$

243 Then, invoking the invariance property of deaggregations, the joint rate is computed by modi-
 244 fying equation (7) to the vector IM case as shown below

$$\lambda(IM_1 > x_1, \dots, IM_n > x_n, M_j, R_j) = P_A(IM_1 > x_1, \dots, IM_n > x_n | M_j, R_j) \lambda(M_j, R_j) \quad (18)$$

245 the vector seismic hazard (which is a normalizing constant in the Bayes' rule application) is
 246 computed by summing equation (18) across all M-R bins

$$\begin{aligned} \lambda(IM_1 > x_1, \dots, IM_n > x_n) &= \sum_{j=1}^{N_{MR}} \lambda(IM_1 > x_1, \dots, IM_n > x_n, M_j, R_j) \\ &= \sum_{j=1}^{N_{MR}} \frac{\sum_{i=1}^{N_s} \lambda_{0i} \sum_{k=1}^{N_M} w_k P(IM_1 > x_1, \dots, IM_n > x_n | M_{jk}, R_{jk}, \hat{p}_{ik}) P(M_{ijk}, R_{ijk})}{\lambda(M_j, R_j)} \lambda(M_j, R_j) \end{aligned} \quad (19)$$

247 which follows the definition of vector seismic hazard while respecting the fault-specific param-
 248 eters for the multiple seismic sources. The above equation is also seen to consider the multiple
 249 branches of a logic tree. Now, the vector deaggregation can be found by dividing equation (18)
 250 by its normalizing constant (equation (19))

$$P(M_j, R_j | IM_1 > x_1, \dots, IM_n > x_n) = \frac{\lambda(IM_1 > x_1, \dots, IM_n > x_n, M_j, R_j)}{\lambda(IM_1 > x_1, \dots, IM_n > x_n)} \quad (20)$$

251 APPLICATION TO A HYPOTHETICAL SITE SURROUNDED BY MULTIPLE FAULT SOURCES

252 To demonstrate the vector deaggregation and hazard at the hypothetical site previously de-
 253 scribed, the IMs Sa(2s) and PGA are considered. The Pearson correlation coefficient between
 254 these two IMs is assumed to be 0.4 (Bradley, 2011). Figure 6a provides a joint aggregated

255 conditional probability of IM exceedences conditioned on an M-R of 7.05-16Km. Figure 6b
 256 provides a vector deaggregation corresponding to a Sa(2s) and PGA pair of 0.5g and 0.75g,
 257 respectively.

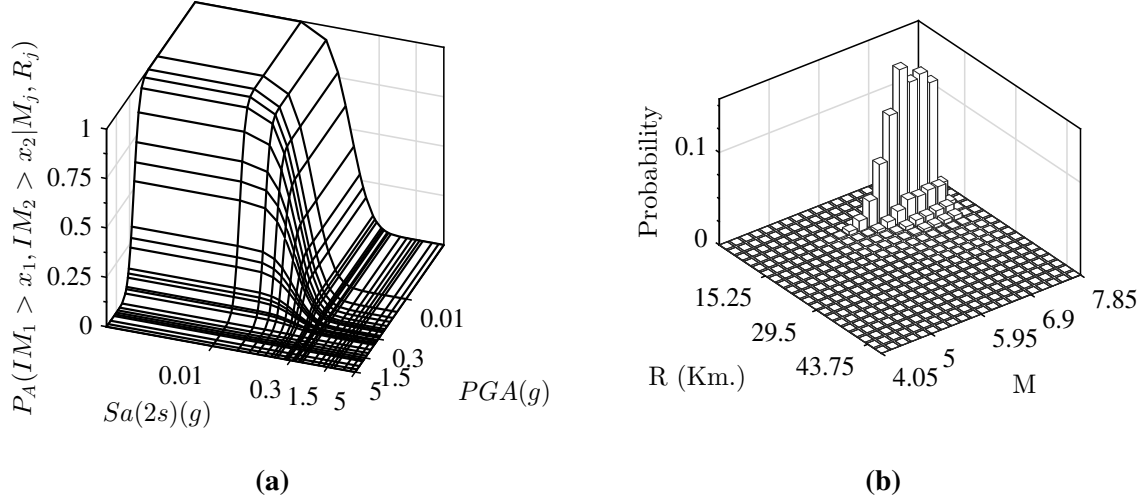


Figure 6. (a) Joint aggregated conditional probability of IM exceedences for the IMs Sa(2s) and PGA conditioned on M-R of (7.05, 16Km) (b) Joint deaggregation corresponding to IM levels of 0.5g and 0.75g for Sa(2s) and PGA, respectively

258 Figure 7 provides the vector hazard surface computed using equation (19). The exact vec-
 259 tor hazard analysis results computed by performing a full Vector PSHA at the hypothetical site
 260 are also provided in this Figure for comparison purposes. It can be noticed that the Copula-
 261 approximated and the exact results are nearly coincident, lending credibility to the proposed
 262 vector hazard approach. To aid a more detailed comparison, Figure 8 provides conditional
 263 hazard curves for $Sa(2s)$ computed using both the Gaussian Copula (solid lines) and the ex-
 264 act vector PSHA (dashed lines). These hazard curves are individually conditioned on PGA
 265 exceedences of $0.25g$, $0.75g$, $2g$, and $5g$. Observing this Figure, it can be concluded that the
 266 Gaussian Copula and the exact results compare very well. Any slight discrepancies, especially
 267 at IM levels of $(Sa(2s) > 5g, PGA > 5g)$, can be attributed to inaccuracies in Gaussian
 268 Copula approximation of the joint aggregated conditional probability of IM exceedences. Other
 269 Copula types, say a ‘ t ’ or a Clayton Copula, can be explored in their capability to more ac-
 270 curately capture the $P_A(IM_1 > x_1, \dots, IM_n > x_n | M_j, R_j)$ and the performance of different
 271 Copula types can be compared. However, such an investigation is outside of the scope of the
 272 present paper and will be treated in a future study; however, an interested reader may refer to
 273 Dhulipala et al. (2018a) for a preliminary investigation on the choice of Copulas.

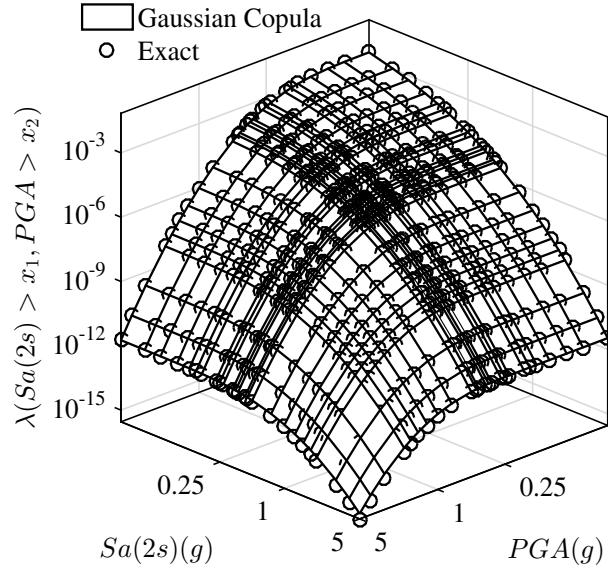


Figure 7. Vector hazard surface for the IMs $Sa(2s)$ and PGA computed using a Gaussian Copula. The exact vector hazard analysis results are also provided for comparison purposes.

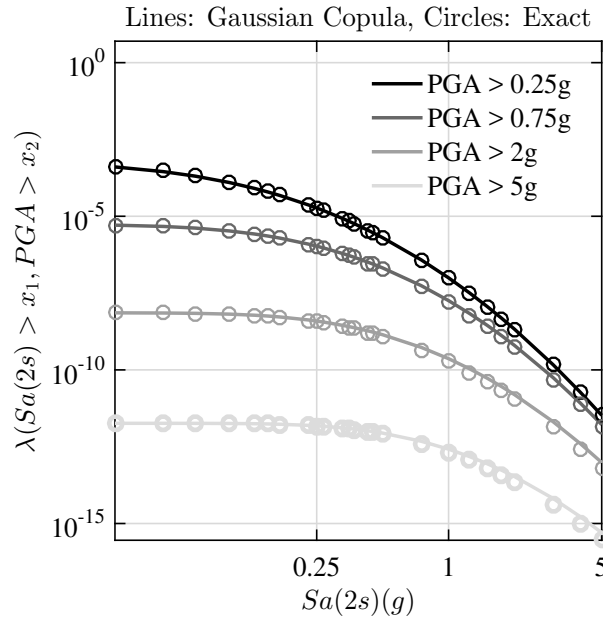


Figure 8. Conditional hazard curves for $Sa(2s)$ computed using both Gaussian Copula (solid lines) and exact vector hazard analysis (circles). These hazard curves are conditioned on PGA exceedences of $0.25g$, $0.75g$, $2g$, and $5g$.

274 Because the joint AFE can be as low as 10^{-15} at this hypothetical site, use of proper nu-
 275 merical accuracy for computations becomes important. We used double precision numerical
 276 accuracy for all our calculations including the exact vector PSHA. In addition, we note that the

277 accuracy of our method for simplified Vector PSHA may depend upon the bin size of deag-
 278 gregation plots with finer discretizations potentially leading to more accurate estimation of the
 279 joint hazard.

280 A sequence of steps required to compute vector deaggregation and vector hazard given the
 281 scalar deaggregations for the various IMs under consideration is shown in algorithm 1.

Algorithm 1 Sequence of steps to compute vector hazard and deaggregation

Require: Vector of IM levels and the correlation matrix between the IMs under consideration

Require: Scalar deaggregations for the vector of IM levels corresponding to different scalar hazard levels

Require: Deaggregation corresponding to a reasonably low IM level (any single IM in the vector of IMs under consideration can be used)

Require: $Total = 0$ (Initialize variable)

- 1: **for** $j = 1 : N_{MR}$ **do**
 - 2: Compute $\lambda(IM > x, M_j, R_j)$ from equation (5) for all the IMs
 - 3: Compute $\lambda(M_j, R_j) = \lambda(IM_{min} > x_{min}, M_j, R_j)$ from equation (5) using the low IM level deaggregation
 - 4: Compute $P_A(IM > x|M_j, R_j)$ and hence $P_A(IM < x|M_j, R_j)$ for all IMs using equations (7) and (12), respectively
 - 5: Compute $P_A(IM_1 < x_1, \dots, IM_n < x_n|M_j, R_j)$ from equation (13) using copulas
 - 6: Compute $P_A(IM_1 > x_1, \dots, IM_n > x_n|M_j, R_j)$ using equation (15)
 - 7: Compute $\lambda(IM_1 > x_1, \dots, IM_n > x_n, M_j, R_j) = P_A(IM_1 > x_1, \dots, IM_n > x_n|M_j, R_j) \lambda(M_j, R_j)$
 - 8: Store(j) $\leftarrow \lambda(IM_1 > x_1, \dots, IM_n > x_n, M_j, R_j)$
 - 9: $Total = Total + \lambda(IM_1 > x_1, \dots, IM_n > x_n, M_j, R_j)$
 - 10: **end for**
 - 11: $\lambda(IM_1 > x_1, \dots, IM_n > x_n) = Total$ (equation (19))
 - 12: $P(M_j, R_j|IM_1 > x_1, \dots, IM_n > x_n) = Store/Total$ (equation (20))
-

282 A MATLAB code which takes scalar deaggregations as inputs and computes vector deaggregation and hazard for
 283 the vector of IM levels considered is provided in software tools.

APPLICATION OF THE PROPOSED VECTOR HAZARD APPROACH TO A REAL SITE IN LOS ANGELES, CA

We apply the proposed vector hazard analysis approach to a real site in Los Angeles, CA [33.996°N; 118.162°W]. The same two IMs, $Sa(2s)$ and PGA , are used for vector hazard computations. OpenSHA software (Field et al., 2003) was used to obtain the scalar hazard curves and the deaggregations at several IM levels using the 2008 Boore and Atkinson GMPM and assuming a V_{s30} of 300 m/s. The *USGS/CGS 1996 Adj. Cal.* Earthquake Rupture Forecast was used for PSHA computations. The deaggregation matrices were discretized to have twenty-four magnitude bins and twenty-three distance bins.

Upon retrieving the scalar hazard curves and deaggregation matrices for the two IMs and their intensities of interest from OpenSHA, the following computations (numbered according to the related step in Algorithm 1) are implemented to compute vector hazard and deaggregation:

2: Given an IM level and an M-R bin in the deaggregation matrix, the joint frequency ($\lambda(IM > x, M_j, R_j)$) is found by multiplying the probability mass of this M-R bin with the seismic hazard of the selected IM level (see equation (5)). Figure 9a depicts $\lambda(IM > x, M_j, R_j)$ as a function of $Sa(2s)$ level at the real site for two M-R bins.

3: The deaggregation matrix corresponding to a low IM level (PGA greater than 0.0001g) is retrieved from the seismic hazard program and used to represent the $\lambda(M_j, R_j)$ for this particular M-R combination (see equation (6)). Figure 9b presents the low-IM-level deaggregation plot at the real site in Los Angeles, CA.

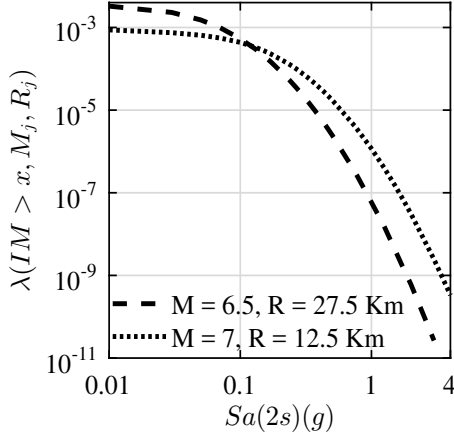
4: For this IM level and M-R bin, the aggregate conditional probability of IM exceedence is found by combining steps (1) and (2) via Bayes' rule (see equation (7)). Figure 9c presents $P_A(IM > x|M_j, R_j)$ as a function of $Sa(2s)$ level for two M-R bins.

6: Given $P_A(IM > x|M_j, R_j)$ for two IMs ($Sa(2s)$ and PGA), the joint aggregate conditional probability of IM exceedences is computed using equations (12) to (16). Figure 9d presents the joint aggregate conditional probability of IM exceedences conditional on an M-R combination 7 – 12.5Km. Although the probability is less than unity for ($Sa(2s) = 0.01g, PGA = 0.01g$), at even smaller IM amplitudes it is expected that $P_A(Sa(2s) > x_1, PGA > x_2|M_j, R_j) = 1$.

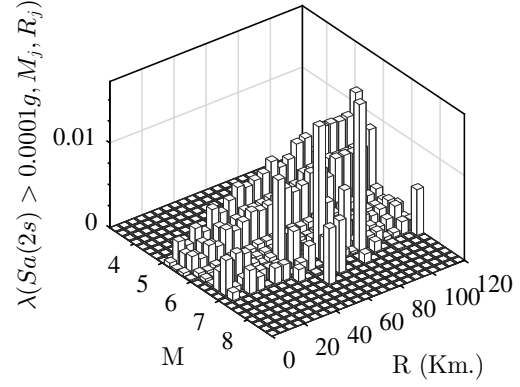
7-12: The joint aggregate conditional probability of IM exceedences given $Sa(2s)$ and PGA levels, and conditional on an M-R combination (step 6), is multiplied with the annual fre-

quency of equivalence of this M-R pair (step 3) and summed across all M-R combinations to compute the vector deaggregation and the vector hazard (see equations (18) to (20)).

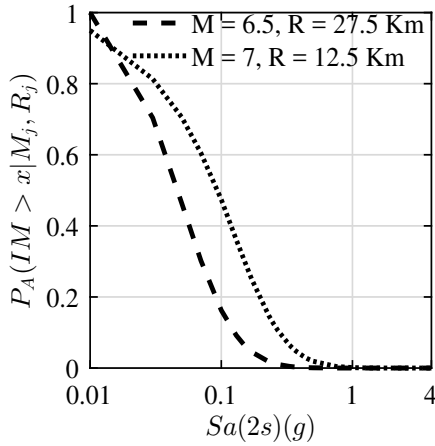
Figure 10 presents the vector hazard surface and the corresponding deaggregation conditional on the IM levels ($Sa(2s) > 0.45g$, $PGA > 0.75g$) at the same site in Los Angeles, CA. It is noted from Figure 10b that deaggregation probabilities are mostly concentrated in two M-R bins at small distances and this behavior should be attributed to nearby fault sources (particularly the Puente Hills fault system) playing a dominant role in controlling the seismic hazard.



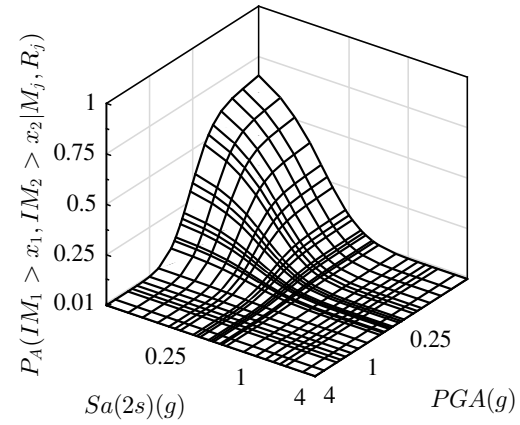
(a)



(b)



(c)



(d)

Figure 9. (a) Depiction of $\lambda(IM > x, M_j, R_j)$ as a function of $Sa(2s)$ level at the real site in Los Angeles, CA for two M-R bins; (b) Low-IM-level deaggregation plot at this site (PGA greater than $0.0001g$); (c) Aggregate conditional probability of IM exceedence as function of $Sa(2s)$ level for two M-R bins at this site; (d) Joint aggregate conditional probability of IM exceedences for the two IMs $Sa(2s)$ and PGA , and conditional on a M-R combination 7 – 12.5Km.

CAN THE INVARIANCE PROPERTY BE UTILIZED TO DIRECTLY COMPUTE SCALAR HAZARD CURVES USING NEW A GMPM/IM?

With the addition of new earthquake records, ground motion databases around the world are constantly expanding and GMPMs are frequently being updated (Boore and Atkinson (2008) to Boore et al. (2014) for example). Moreover, many advanced IMs have been proposed that intend to capture multiple aspects of ground motion and that have been shown to better pre-

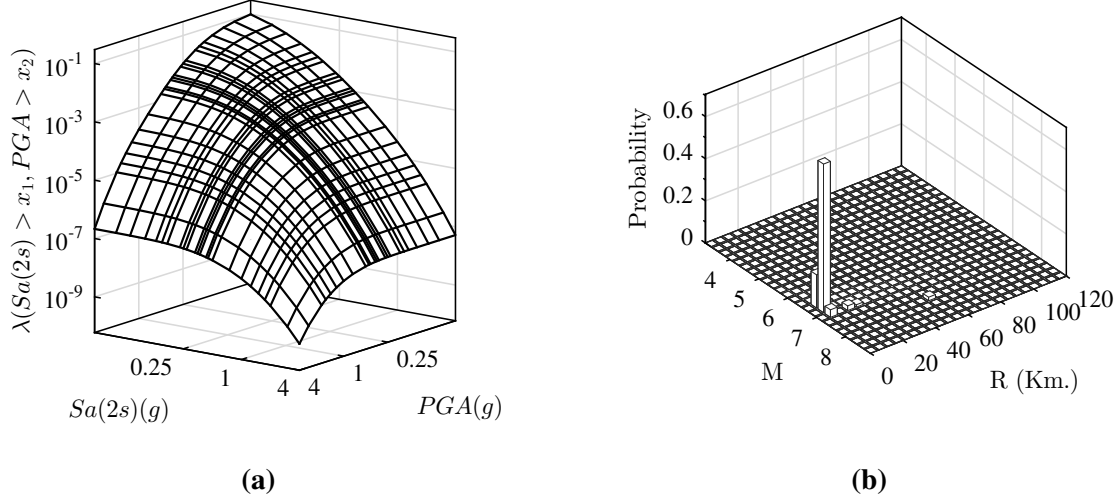


Figure 10. (a) Vector hazard surface and the (b) Corresponding deaggregation conditional on the IM levels ($Sa(2s) > 0.45g$, $PGA > 0.75g$) at the same site in Los Angeles, CA.

dict structural response than conventional IMs (such as $Sa(T_1)$; see Marafi et al. (2016) for example). Within the framework of Performance Based Earthquake Engineering, these new GMPMs or IMs are only useful if their seismic hazard curves are available, which would in general require re-programming PSHA software to include these new GMPMs/IMs. If preliminary PSHA results could be obtained with less effort it would support the rapid assessment of candidate IMs, e.g., evaluation of their efficiency and sufficiency (Dhulipala et al., 2018b). This section therefore explores whether the properties of scalar hazard deaggregations can be leveraged to estimate scalar hazard curves using new GMPMs/IMs.

The invariance property of deaggregations is convenient in that it directly represents the relative importance of different M-R combinations without regard to the IM in terms of a frequency ($\lambda(M_j, R_j)$). Given an M-R combination, the probability of exceedence of an IM level ($P(IM > x|M_j, R_j)$) can be computed using the new GMPM or by fitting a GMPM to the new IM. Then, the seismic hazard curve can directly be computed without performing a full PSHA for the new IM using,

$$\lambda(IM > x) = \sum_{j=1}^{N_{MR}} P(IM > x|M_j, R_j) \lambda(M_j, R_j) \quad (21)$$

which is exact only if $P(IM > x|M_j, R_j)$ is equal to the aggregated conditional probability of IM exceedence. As mentioned earlier in the discussion related to equation (11), $P(IM >$

$x|M_j, R_j)$ and $P_A(IM > x|M_j, R_j)$ are equivalent only if a single GMPM is used in the logic tree and this GMPM does not take into account source related parameters. Contemporary GMPMs, however, require at least the type of the fault as an input, with more complicated GMPMs, such as CB2008, requiring other parameters such as Z_{tor} , Z_{vs} , λ , and δ (refer to Table 1 for abbreviations).

The quality of the approximation made by equation (21) to compute the seismic hazard of a scalar IM will be tested by assuming that the Boore and Atkinson (2008) with an unspecified fault type is a new GMPM or a GMPM fitted to a new IM. Then, the computed hazard curve will be compared with the one obtained from OpenSHA using the same GMPM but considering the fault-specific characteristics. Figures 11a and 11b provide seismic hazard curves at the same site in Los Angeles, CA for the IMs $Sa(2s)$ and PGA from OpenSHA along with the approximate hazard curves from equation (21). Given the low effort required in terms of not having to re-run hazard calculations or having to re-program the PSHA software to include the new IM/GMPM, the approximate hazard curve makes a reasonable prediction of the seismic hazard up to an IM level $0.5g$ for both $Sa(2s)$ and PGA . After $0.5g$, however, the approximate curve starts to deviate from the exact one and this effect is seen to be more prominent for PGA . So, the hazard curve obtained from equation (21) can only be considered as a preliminary approximation and it needs to be further tested for other sites and IMs. However, for a preliminary seismic risk assessment of structures using advanced IMs or new GMPMs whose seismic hazard curves are unavailable from PSHA programs, the approximate procedure for scalar hazard estimation proposed in this section can be employed.

SUMMARY AND CONCLUSIONS

Vector PSHA is computationally expensive and requires substantial modification of existing PSHA programs to perform the calculations in an exact sense. In this paper, we described a computationally inexpensive procedure to compute vector -hazard and -deaggregation that only relies on the outputs from existing PSHA programs: scalar hazard curves and M-R deaggregation matrices. Three key properties of scalar deaggregations were first identified: a) they monotonically decrease with IM level; b) they are invariant to the choice of IM for a low IM level; and c) each M-R bin is part of a CCDF, termed the aggregated conditional probability of IM exceedence. We then utilized these properties of deaggregations along with Copulas to compute vector -hazard and -deaggregation given a suite of IMs in a simplified fashion. The nature of the approximation made by our simplified approach was investigated by performing

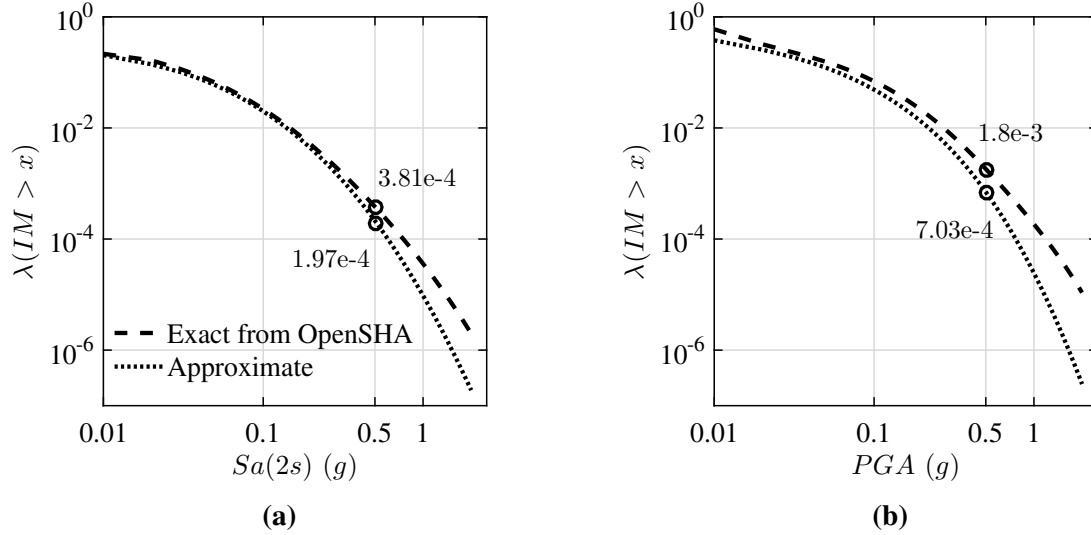


Figure 11. Comparison of hazard curve from OpenSHA with an approximate one obtained using the invariance property of deaggregations for the IMs (a) $Sa(2s)$ and (b) PGA . These plots are for the same site in Los Angeles, CA.

and comparing to the results of an exact vector PSHA using a logic-tree at a hypothetical site surrounded by two fault sources. We find that at this hypothetical site our simplified method for vector hazard gave very good approximations. Additionally, we demonstrate the application of our approach to Vector PSHA at a real site in Los Angeles, CA, using the PSHA program OpenSHA.

Our approach for simplified computation of vector PSHA accounts for logic-tree and multiple fault sources (routinely considered in modern PSHA computations) while taking as inputs only the basic quantities such as scalar hazard curve and M-R deaggregations. As a result, we anticipate that our method will be valuable given that modern GMPMs may account for more fault-specific parameters and PSHA may consider more epistemic uncertainty through logic-tree in the future.

Finally, we also provide a discussion on how the invariance property of deaggregations can be used to compute hazard curves for new GMPMs or GMPMs fitted to new IMs. The computed hazard curve is only exact if a single GMPM is used in logic trees and this GMPM does not account for earthquake source related parameters. However, for the IMs and the site considered in this study, we obtain reasonable predictions for low to moderate values of the IM.

SOFTWARE TOOLS

A MATLAB code which takes scalar deaggregations as inputs and computes vector deaggregation and hazard for the vector of IM levels considered is available at:

https://github.com/somu15/Vector_Hazard_and_Deaggregation

ACKNOWLEDGEMENTS

This research is supported by the US National Science Foundation, Division of Civil, Mechanical, and Material Innovation, through award number 1455466 under the Resilient and Sustainable Buildings program. Additional support for the first author was provided by the Virginia Tech College of Engineering Pratt fellowship. We thank Dr. Jack Baker and an anonymous reviewer for their valuable comments that have improved the paper's quality.

APPENDIX: DISCUSSION ON THE INTENSITY MEASURE CORRELATION COEFFICIENTS IN RELATION TO THE PROPOSED VECTOR HAZARD APPROACH

The proposed procedure for simplified vector hazard analysis makes the use of Copula functions that require the aggregated conditional probabilities of IM exceedence ($P_A(IM > x|M_j, R_j)$) for the IMs considered and correlations between these IMs as inputs. This appendix provides a discussion on the use of IM correlations derived using a single GMPM to compute the aggregated conditional probabilities of multiple IM exceedences ($P_A(IM_1 > x_1, \dots, IM_n > x_n|M_j, R_j)$) via Copulas.

The quantity $P_A(IM > x|M_j, R_j)$ can include multiple GMPMs weighted through a logic-tree (see Figure 1). The computation of $P_A(IM_1 > x_1, \dots, IM_n > x_n|M_j, R_j)$, however, utilizes the IM correlation coefficients derived through a single GMPM. To explore the adequacy of this disparity between the GMPMs used in the logic-tree and the GMPM adopted for computing IM correlations, two case-studies are considered. The first study considers a subset of the NGA-West2 database^{c)} (Ancheta et al., 2014), and two corresponding GMPMs BA2008 and CB2008. The second study considers a subset of the NGA-East database^{d)} (Goulet et al., 2014), and two corresponding GMPMs Atkinson and Boore 2006 (AB2006) and Shahjouei and

^{c)}496 recordings for which the Z_{vs} value is available were used.

^{d)}320 recordings on rock sites were used.

420 Pezeshk 2016 (SP2016). For both these case-studies, the correlations between PGA and SA
 421 are first computed using a single GMPM. Next, these correlations are computed using the two
 422 GMPMs by assigning weights to replicate the logic-tree. Finally, the different correlation values
 423 will be compared.

424 IM correlations are computed by first determining the ε values. ε is defined as:

$$\varepsilon_i = \frac{\ln IM_i - \mu_{IM_i}}{\sigma_i} \quad (22)$$

425 where IM_i is the i th IM recording from the database, μ is the predicted IM value using a
 426 GMPM, and σ is the standard deviation of this prediction. When two GMPMs are utilized by
 427 assigning weights (w^1 and w^2 , respectively), the mean prediction and the standard deviation are
 428 computed using:

$$\begin{aligned} \mu_{IM_i}^* &= w^1 \mu_{IM_i}^1 + w^2 \mu_{IM_i}^2 \\ \sigma_i^* &= \sqrt{w^1 (\sigma_i^1)^2 + w^2 (\sigma_i^2)^2} \end{aligned} \quad (23)$$

429 where $(\mu_{IM_i}^1, \sigma_i^1)$ and $(\mu_{IM_i}^2, \sigma_i^2)$ are the mean and standard deviation pairs for the two GMPMs
 430 adopted, respectively, and the super-script $(.)^*$ represents a combined mean or standard devi-
 431 ation. The PGA, SA correlations computed considering the two GMPMs separately and in a
 432 combined fashion are presented in Figure 12.

433 From Figure 12a, it is noted that while considering the NGA-West2 database, the PGA, SA
 434 correlations are not significantly affected by the GMPM adopted. Consequently, the correla-
 435 tions obtained from weighting the GMPMs are also quite consistent with the individual GMPM
 436 results. However, when considering the NGA-East database (Figure 12b), the correlations are
 437 influenced by the GMPM adopted. Hence, while applying the proposed method for vector haz-
 438 ard, caution needs to be exercised while using the IM correlation coefficients for the Copula
 439 functions. For the NGA-West2 database, mean predictions from different GMPMs were ob-
 440 served to be close. So, the computed IM correlations may not be significantly impacted by the
 441 choice of GMPM. On the other hand, for the NGA-East and subduction zone databases, mean
 442 predictions may not be consistent across the GMPMs. Consequently, the IM correlations, as
 443 shown in Figure 12b, can be quite different.

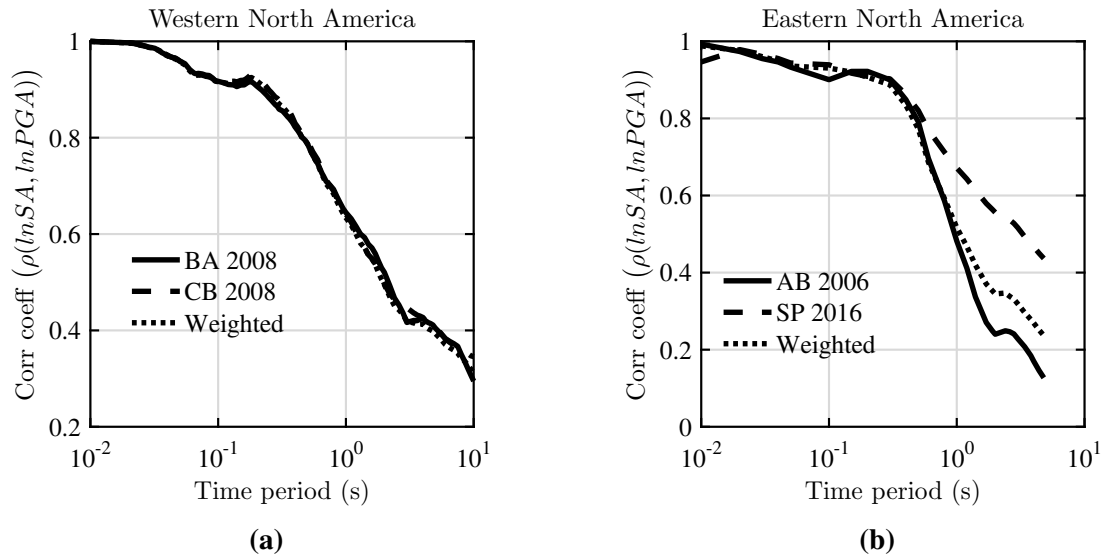


Figure 12. PGA, SA correlations computed using the: (a) NGA-West2 and (b) NGA-East databases. It is noted that the correlations are computed using a subset of these databases and are not recommended for use in practice.

REFERENCES

- 444
- 445 Ancheta, T. D., Darragh, R. B., Stewart, J. P., Seyhan, E., Silva, W. J., Chiou, B. S., Wooddell, K. E.,
 446 Graves, R. W., Kottke, A. R., Boore, D. M., Kishida, T., and Donahue, J. L., 2014. NGA-West2
 447 database. *Earthquake Spectra* **30**, 989–1005.
- 448 Atkinson, G. M. and Boore, D. M., 2006. Earthquake ground-motion prediction equations for eastern
 449 North America. *Bulletin of the Seismological Society of America* **96**, 2181–2205.
- 450 Baker, J. W. and Bradley, B. A., 2017. Intensity Measure Correlations Observed in the NGA-West2
 451 Database, and Dependence of Correlations on Rupture and Site Parameters. *Earthquake Spectra* **33**,
 452 145–156.
- 453 Barbosa, A. R., 2011. Simplified vector-valued probabilistic seismic hazard analysis and probabilistic
 454 seismic demand analysis : application to the 13-story NEHRP reinforced concrete frame-wall building
 455 design example. Ph.D. thesis, University of California, San Diego.
- 456 Bazzurro, P. and Cornell, A. C., 1999. Disaggregation of seismic hazard. *Bulletin of the Seismological*
 457 *Society of America* **89**, 501–520.
- 458 Bazzurro, P. and Cornell, A. C., 2002. Vector-valued probabilistic seismic hazard analysis. In *Seventh*
 459 *U.S. National Conference on Earthquake Engineering*. Boston, MA.
- 460 Bazzurro, P. and Park, J., 2011. Vector-valued probabilistic seismic hazard analysis of correlated ground
 461 motion parameters. In *Applications of Statistics and Probability in Civil Engineering*, pp. 1596–1604.
- 462 Bazzurro, P., Tothong, P., and Park, J., 2009. Efficient approach to vector-valued probabilistic seismic
 463 hazard analysis of multiple correlated ground-motion parameters. In *International Conference On*
 464 *Structural Safety And Reliability*. Osaka, Japan.
- 465 Boore, D. M. and Atkinson, G. M., 2008. Ground-motion prediction equations for the average hori-
 466 zontal component of PGA, PGV, and 5%-damped PSA at spectral periods between 0.01 s and 10.0 s.
 467 *Earthquake Spectra* **24**, 99–138.

- Boore, D. M., Stewart, J. P., Seyhan, E., and Atkinson, G. M., 2014. NGA-West2 Equations for Predicting Response Spectral Accelerations for Shallow Crustal Earthquakes. *Earthquake Spectra* **30**, 1057–1085.
- Bradley, B. A., 2011. Empirical correlation of PGA, spectral accelerations and spectrum intensities from active shallow crustal earthquakes. *Earthquake Engineering & Structural Dynamics* pp. 1707–1721.
- Bradley, B. A., 2012. Empirical correlations between peak ground velocity and spectrum-based intensity measures. *Earthquake Spectra* **28**, 17–35.
- Campbell, K. W. and Bozorgnia, Y., 2008. NGA ground motion model for the geometric mean horizontal component of PGA, PGV, PGD and 5% damped linear elastic response spectra for periods ranging from 0.01 to 10 s. *Earthquake Spectra* **24**, 139–171.
- Dhulipala, S. L. N., Rodriguez-Marek, A., and Flint, M. M., 2018a. Salient Features of Seismic Hazard Deaggregation and Computation of Vector Hazard. In *Geotechnical Earthquake Engineering and Soil Dynamics V*. Denver, Colorado.
- Dhulipala, S. L. N., Rodriguez-Marek, A., Ranganathan, S., and Flint, M. M., 2018b. A site-consistent method to quantify sufficiency of alternative IMs in relation to PSDA. *Earthquake Engineering & Structural Dynamics* **47**, 377–396.
- Field, E. H., Jordan, T. H., and Cornell, A. C., 2003. OpenSHA: A Developing Community - Modeling Environment for Seismic Hazard Analysis. *Seismological Research Letters* **74**, 406–419.
- Goda, K. and Atkinson, G. M., 2009. Interperiod dependence of ground-motion prediction equations: A copula perspective. *Bulletin of the Seismological Society of America* **99**, 922–927.
- Goulet, C. A., Kishida, T., Ancheta, T. D., Cramer, C. H., Darragh, R. B., Silva, W. J., Hashash, Y. M. A., Harmon, J., Stewart, J. P., Wooddell, K. E., and Youngs, R. R., 2014. *PEER NGA-East database. Tech. rep.*, Pacific Earthquake Engineering Research.
- Hoff, P., 2009. *A first course in Bayesian statistical analysis*. 1st edn. Springer, Seattle, 1–270 pp.
- Kohrangi, M., Bazzurro, P., and Vamvatsikos, D., 2016a. Vector and Scalar IMs in Structural Response Estimation: Part I Hazard Analysis. *Earthquake Spectra* **32**.
- Kohrangi, M., Bazzurro, P., and Vamvatsikos, D., 2016b. Vector and Scalar IMs in Structural Response Estimation, Part II: Building Demand. *Earthquake Spectra* **32**.
- Kramer, S., 1996. *Geotechnical earthquake engineering*. Prentice Hall, New York.
- Kwong, S. N. and Chopra, A. K., 2016. A Generalized Conditional Mean Spectrum and its application for intensity-based assessments of seismic demands. *Earthquake Spectra* **33**, 1–28.
- Lin, T., 2012. Advancement of hazard-consistent ground motion selection methodology. Ph.D. thesis, Stanford University.
- Marafi, N., Berman, J., and Eberhard, M., 2016. Ductility-dependent intensity measure that accounts for ground- motion spectral shape and duration. *Earthquake Engineering & Structural Dynamics* pp. 653–672.
- Shahjouei, A. and Pezeshk, S., 2016. Alternative hybrid empirical ground-motion model for central and Eastern North America using hybrid simulations and NGA-West2 models. *Bulletin of the Seismological Society of America* **106**, 734–754.